Spinodal decomposition of a confined colloid-polymer system

E. A. G. Jamie, R. P. A. Dullens, and D. G. A. L. Aarts[a)]
Department of Chemistry, Physical and Theoretical Chemistry Laboratory, University of Oxford, South Parks Road, Oxford OX1 3QZ, United Kingdom

(Received 9 August 2012; accepted 29 October 2012; published online 27 November 2012)

We study the demixing via spinodal decomposition of a fluid-fluid phase separating colloid-polymer mixture confined between parallel plates, where one of the phases completely wets both walls. Using confocal scanning laser microscopy, we are able to obtain real space images, both parallel and perpendicular to the cell walls. We observe three distinct morphologies: the formation of a bicontinuous network, which coarsens into cylindrical tubes bridging the plates, and finally develops into a network structure in two dimensions. Through image analysis of the system as a whole, and the tracking of individual domains, we are able to perform a detailed study of the mechanisms of phase coarsening at each stage. We are able to directly test the condition for which bridges connecting both confining walls do not sever. Finally, we consider the role of hydrodynamics and of thermal interface fluctuations in our system. © *2012 American Institute of Physics*. [http://dx.doi.org/10.1063/1.4767399]

I. INTRODUCTION

The phase behaviour of fluids confined between two or more surfaces is of fundamental scientific interest, and shows complex dynamics of patterns. There is also a clear industrial/technological relevance; controlling fluid interfaces at decreasing lengthscales leads to novel structures and therefore textures, important to, for example, the food industry.[1] In addition to the interaction between phase separation and the preferential wetting of a surface by one component in the system,[2–4] finite size effects (e.g., capillary condensation) due to the finite width of the confinement geometry[5–8] may also play a role. The combination of surface geometry and interfacial tension in the system may create new stable or metastable structures such as capillary bridges,[9,10] and the presence of the confining walls may cause phase transitions to occur not seen in the bulk,[11–13] or change the dimensionality of the phase separation.[14]

The dynamics of a bulk system demixing via the spinodal decomposition mechanism are well established.[15–18] In the initial stage, density fluctuations governed by the free energy landscape grow in amplitude at a wavelength independent of time, known as the linear Cahn Hilliard regime.[19] The system then moves into a diffusive regime, where the characteristic lengthscale L coarsens as a function of time t with a power law of $L(t) \sim t^{1/3}$ followed by a viscous hydrodynamic regime, where $L(t) \sim t^{1}$.[15] This may be followed by an intertial regime.[20] When the domain size becomes comparable to the capillary length of the system, buoyancy forces will rip apart the structures and the phase separation will become driven by gravity.[15]

When the system demixes in the vicinity of a surface, which is preferentially wet by one of the phases, an oscillating density wave will propagate perpendicular to the surface into the bulk, breaking the symmetry of the domains.[2,3,21–23] This phenomenon is known as surface directed spinodal decomposition (SDSD). For fluid-fluid phase separations, this morphology consists of a wetting layer of the preferred phase on the surface, then a further (depletion) layer of the non-preferred phase,[24] possibly followed by additional alternating layers, depending on the strength of the surface field and the depth of the quench.[4,25–28] In a system confined by two walls in one dimension, but unrestricted in the other two, density oscillations will propagate perpendicular to each surface. Depending on the spacing between the plates, these waves may overlap and interfere. In case of extreme confinement, this picture breaks down and a new wavelength, which depends on the slit width, is imposed on the system.[29,30]

We next discuss the case of a system roughly symmetric in composition, which demixes via spinodal decomposition between two confining surfaces. Both surfaces are assumed to be completely wet by the same phase. The three-dimensional growth of domains is limited by the presence of the surfaces and the morphology and dynamics of phase coarsening is dramatically affected by the interaction with the wetting layers.[31–33] Previous studies in polymeric systems divide the phase separation process into three stages;[14,25,33] similar observations have been made in simulations.[34] For spinodal decomposition, the system progresses as in bulk through the early stage regimes into the linear hydrodynamic regime, and a three dimensional interconnected network structure with sharp interfaces is formed (*first stage*). The wetting layers are connected to the spinodal network, enabling transport of the wetting phase to the surfaces via a hydrodynamic process.[15,35]

As the demixing progresses, the three dimensional network coarsens into a system of two dimensional bridging tubes between the plates,[14,25,33] characterizing the beginning of the *second stage* of demixing. The subsequent behaviour of the bridging tube is dependent on its size. The Laplace pressure directs the flow of material either into the wetting layers, or into the bridging tube depending on the relative radii of curvature of the two dimensional domain. Bridges are predicted to expand if their radius r is larger than half the plate spacing d, i.e., $r > d/2$.[32,36] Smaller bridges will shrink, eventually

a)Electronic mail: Dirk.Aarts@chem.ox.ac.uk.

running out of material and the connection between the two layers will break.[14,36] For bridges wider than this critical radius, the diameter of the circular domain is predicted to grow linearly in time, due to the hydrodynamic transport of matter from the wetting layer to the bridging tube.[23,36]

In the *third stage*, domain growth slows down as the wetting layers run out of material and further coarsening of the system becomes driven by the diffusion and coalescence of bridging tubes. The system converts to an interconnected network morphology characterizing the third stage.[25,32,33,36]

In this work, we study demixing between two parallel plates of a system of colloids and non-adsorbing polymers, which phase separate from the unstable region of the phase diagram. The origin of the phase separation is an attractive depletion interaction between the colloids, driven by the polymers.[37,38] This results in the formation of a colloid-rich, polymer-poor colloidal "liquid" phase, and a polymer-rich, colloid-poor colloidal "gas" phase.[39] The large size of the colloids means the interfacial tension γ associated with the interface separating the two phases is many orders of magnitude smaller than in a molecular system: $\gamma \sim \mathcal{O}(\mathrm{nN/m})$ instead of $\mathcal{O}(\mathrm{mN/m})$. This leads to favorable length and timescales, and allows a detailed study of demixing in bulk[18,40] and in confinement/at single surfaces.[28,41] In previous studies, we have given a detailed account of the phase separation in the vicinity of a single surface[28] and also in confinement,[41] but in the case where droplet diffusion and coalescence are important/dominant. In the present study, the morphology is completely different and the phenomenology is inherently more complex and rich. We will explore the phase separation of our system in both the parallel and perpendicular directions to the surfaces. High resolution images allow the detailed analysis of domain behaviour, and we explore the mechanisms of phase coarsening as the system passes through the stages described above.

We begin by describing our experimental and analysis methods in Sec. II, before presenting our results in Sec. III, and interpreting our findings in the light of previous studies. In Sec. IV, we will conclude.

II. EXPERIMENTAL METHODS AND ANALYSIS

A dispersion of fluorescently labelled PMMA particles in water was prepared using the first part of the emulsion polymerization method described by Kumacheva *et al.*[42] The spherical colloidal particles were characterised using scanning electron microscopy and found to be of radius $R_c = 110$ nm and low polydispersity, corroborated by the fact that samples spontaneously crystallized. A solution of xanthan polymer (molecular weight $M_w = 4 \times 10^6$ g mol^{-1}, radius of gyration $R_g = 264$ nm) was prepared as described in Ref. 43. Combining these two components in the appropriate concentrations gave a fluid-fluid phase separating mixture.[44] The solvent of a stock solution of colloids was converted to a mixture of approximately 23% water and 77% glycerol by repeated centrifugation. The added glycerol generally slowed down the phase phase separation progress.[40] The overall volume fractions were $\phi_c = \frac{4}{3}\pi R_c^3 n_c = 0.14$ and $\phi_p = \frac{4}{3}\pi R_G^3 n_p = 2.33$ with $n_{c/p}$ the number densities of colloids or polymers, respectively. Furthermore, after phase separation had completed the colloidal liquid-colloidal gas ratio was 70:30 in bulk. The density difference between the two phases was small, of the order of 1 kg/m^3, estimated from additional experiments on the thermal capillary waves at the interface.

The sample was homogenised using a vortex, and phase separations were recorded in real space using confocal scanning laser microscopy (CSLM; Zeiss Exciter). Bulk phase separation was imaged using a 10× magnification lens in the direction parallel to both gravity and the cell wall. As in our previous bulk studies,[40] we used a glass container with dimensions chosen to minimise solvent flow, but not confine the system.

The confined phase separations took place in open ended polydimethyl siloxane (PDMS) microfluidic channels, constructed as described in Refs. 45 and 46. These were approximately 18 μm in height ($d = 18$ μm) and the other two dimensions were greater than 1 mm such that the system is only confined in one direction, parallel to gravity. After the sample was homogenised, the cell was filled by capillary action. The demixing of the sample was imaged in both the *xz* plane (perpendicular to the plates) and *xy* plane (parallel to the plates). In the *xz* plane, we used a 63× magnification lens to study a slice away from any vertical confining edge, and in the *xy* images we focused to a central plane parallel to the walls using a 10× magnification lens. After a few hours, the sample began to dry, which was before full equilibrium was reached, but the final stage in the phase separation process had already been reached.

The coarsening rate of domains in the bulk and in the *xy* plane of the confined systems were determined by performing 2-dimensional discrete Fourier transforms (FFT) on the CSLM images.[18,47] The structure factors, $I(k, t)$, where I is the intensity of the image and k is the wavevector, were obtained by radially averaging the Fourier transforms. The wavevector at the maximum intensity $I_{max} \equiv I(k_{max}, t)$ was obtained by fitting a Gaussian curve to the data. The correlation length in the system corresponds to $L = L_{image}/k_{max}$, where L_{image} is the image width and the coarsening rate in the systems is obtained by plotting L against time.

Further analysis of the images in the *xy* plane was performed using standard image analysis routines on binarised images in Mathematica 8. This provided for a single plane the centre of mass and area of each domain, in addition to the total number and area fraction of all domains combined. The domain radius r was calculated using the basic formula $area = \pi r^2$, which stops working for non-circular domains. The behaviour of individual domains was monitored in time using standard particle tracking software in Interactive Data Language (IDL),[48] allowing the path and growth of individual domains to be followed.

III. RESULTS AND DISCUSSION

Before investigating the behaviour of the sample in confinement, we establish the dynamics of bulk demixing. The

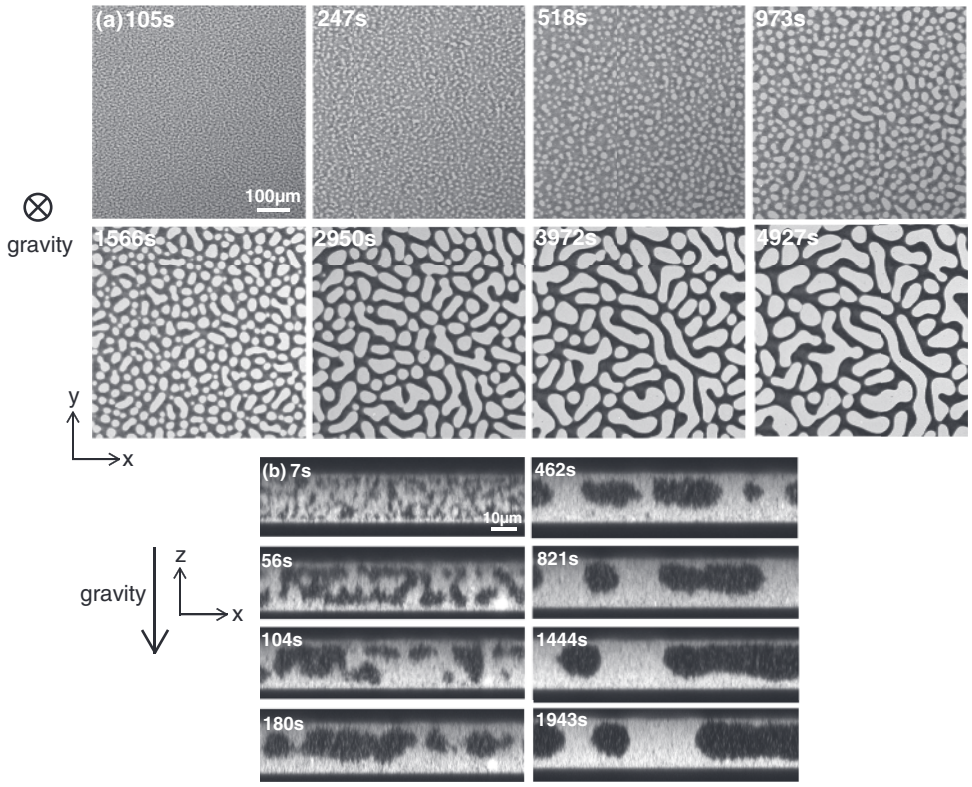

FIG. 1. CSLM images of the phase separation in an 18 μm wide cell. The upper images are in the *xy* plane, and the lower images in the *xz* plane. The bright phase is the colloidal liquid, and the dark phase the colloidal gas.

sample exhibits the characteristic bicontinuous spinodal network morphology, see also Ref. 40 for bulk studies on very similar systems. By examining the coarsening rate of domains obtained from FFT analysis, we ascertain that the system progresses through the initial spinodal regimes in a matter of seconds, before coarsening in the linear hydrodynamic regime for around 10 min. The lengthscale diverges at a size of approximately 50 μm as domains are ripped apart by buoyancy forces. We thus expect that by confining our sample to 18 μm in the direction of gravity, gravity will only play a very small role in the coarsening of our sample. We will now first give a qualitative account of the demixing in confinement, followed by a quantitative description.

A. Qualitative description

CSLM images of the phase separation in confinement between parallel plates are shown in Figure 1. It is immediately clear that the liquid (bright) phase completely wets both the glass (lower) and PDMS (upper) surfaces (Figure 1(b)), which given the underlying depletion interaction are expected to behave identical. In the *first stage*, we observe a thin layer of the liquid phase immediately coating both surfaces. A bicontinuous spinodal network forms between the plates, connecting the wetting layers (Figures 1(a) 105 s, 1(b) 7−104 s). As the system coarsens, the tube structure of the spinodal network widens, and the wetting layers thicken as material is transported from the central network to the surfaces. The presence of the surfaces prevents the domains growing symmetrically in three dimensions, so the network structure transforms into a set of cylindrical tubes connecting the two wetting layers (Figures 1(a) 247 s, 1(b) 56−180 s), thus entering the *second stage* in the phase separation process. In the *xy* plane, the cross sections of these bridges appear as bright spots, and signify the transformation of the 3D spinodal network to a 2D system of circular bridges.

As demixing progresses, the larger bridges grow in diameter, whereas the smaller ones shrink, until their connections between the plates sever (Figure 1(a) 247−973 s). In the *xz* plane, we see that as long as the structure is a 3D network, the wetting layers thicken (Figure 1(b) 56−180 s), but once the system becomes a set of circular bridges expanding in the *xy* plane, the wetting layers thin again (Figure 1(b) 462−1943 s). This illustrates the reversal of the direction of flow. When the wetting layer is connected to the spinodal network, the Laplace pressure directs the flow of the liquid phase into the wetting layers. Once large bridges of diameter greater than the plate spacing have been established, the pressure gradient changes direction, and the bridges grow as they feed on the wetting layer. The bridges begin to collide after around 1100 s and structures grow by diffusion and coalescence, which characterizes the *third stage* of demixing. The domains attempt to regain a circular shape to minimise their interfacial area, however collisions are frequent and the morphology becomes partially interconnected (Figure 1(a) 973−2950 s). In the *xz* images (Figure 1(b) 180−1943 s), we observe that the wetting layer on the lower surface is somewhat thickened, and the meniscus (in the plane perpendicular to the walls) is slightly asymmetrical, see Ref. 49 for a detailed study of this shape. This illustrates a small effect of gravity on demixing, consistent with the plate spacing being slightly larger than the capillary length within the system.[32]

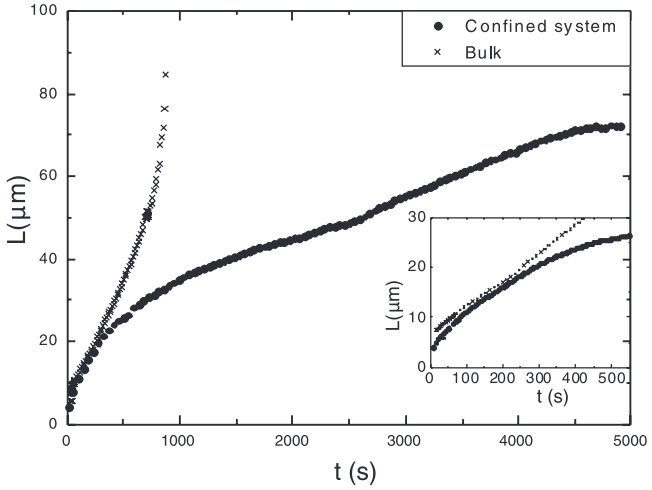

FIG. 2. Comparison of the FFT analysis of bulk and confined samples in the *xy* plane. The inset highlights coarsening behaviour at early times.

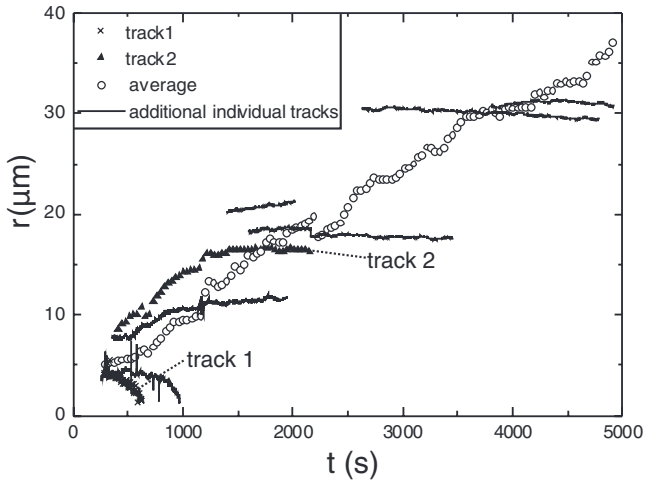

FIG. 4. Plot of domain radius vs. time for various individually tracked domains. Tracks 1 and 2 are discussed in more detail in the text and correspond to Figures 3 and 5. The additional individual tracks are for illustration. The average domain radius is shown as well.

B. Quantitative description

We shall now quantify our observations through the analysis of our CSLM images. During the first stage, the confined system displays a 3D bicontinuous network structure with thickening wetting layers. Figure 2 shows that the characteristic lengthscale of the confined system (obtained by the FFT analysis) coarsens at a similar rate to that of the bulk. In this first stage, where domains are smaller than the plate spacing, we expect the dynamics of the system to follow SDSD.[29,30,34] We expect the system to cross over from a diffusive $\sim t^{1/3}$ to a viscous hydrodynamic $\sim t^{1}$ coarsening regime, just as in bulk. The additional curvature for the confined data at early times in Figure 2 suggests that the crossover is slower than in bulk. After around 250 s, at which time the domain correlation lengthscale is comparable to the plate spacing and the morphology of the phase separation is changing to a system of circular bridging tubes, the coarsening rate of the system begins to deviate significantly from that in the bulk.

The appearance of bridging tubes between the plates shows that the system is crossing over from the first to the second stage. From $t \sim 280$ s onwards, we are able to identify individual domains and track them using the Mathematica software (we set a minimum area for detection equivalent to a circle with radius $r = 1.2\ \mu$m). In Figure 3, we show an example of such a domain, its centre of mass is indicated by a cross. We follow its position and radius in time, and plot its size in Figure 4 (labelled track 1). As the radius of the tube is smaller than $d/2$ ($= 9\ \mu$m; see also the discussion around Figure 6),

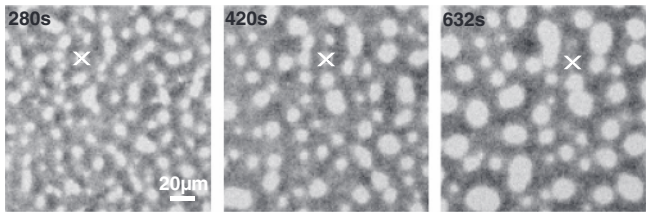

FIG. 3. Tracking of track 1. The centre of mass of the domain is marked by an x.

the Laplace pressure directs material out of the tube and into the wetting layer, and we indeed see the tube shrink. Shortly after the final image, we lose the track as the tube becomes smaller than the minimum detection area, and the connection between the two layers severs.

When two tubes collide and form a new single tube with a significantly different centre of mass, the tracks of the two original domains are lost and a new track corresponding to the new domain is begun. We illustrate this in Figure 5. In the first image, the track begins as the centre of mass between two colliding bridging domains. Again the position of the centre of mass of the tracked domain is marked with a cross. The domain changes its shape to become circular and minimise its interfacial area. As the radius of the tube is greater than $d/2$, the Laplace pressure directs material from the wetting layer into the tube, and its radius expands. At later times, as the wetting layers thin and run out of material, the growth of the tube radius slows considerably. We plot the domain radius as a function of time in Figure 4 (labelled track 2). In the frame

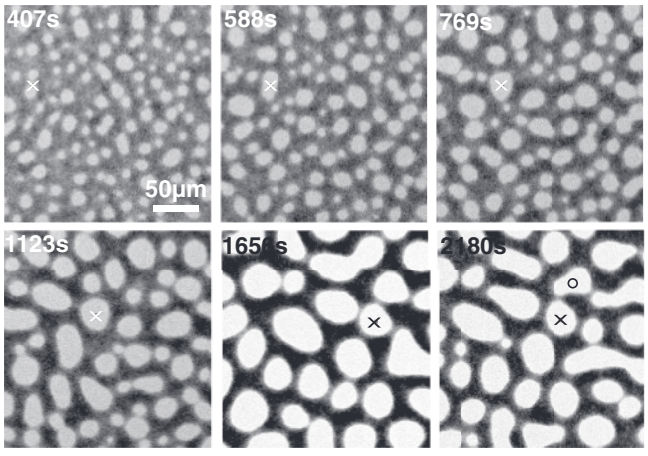

FIG. 5. Tracking of track 2. The centre of mass of the domain is marked by an x. The track is lost after the final image as the domain collides with another marked by a circle.

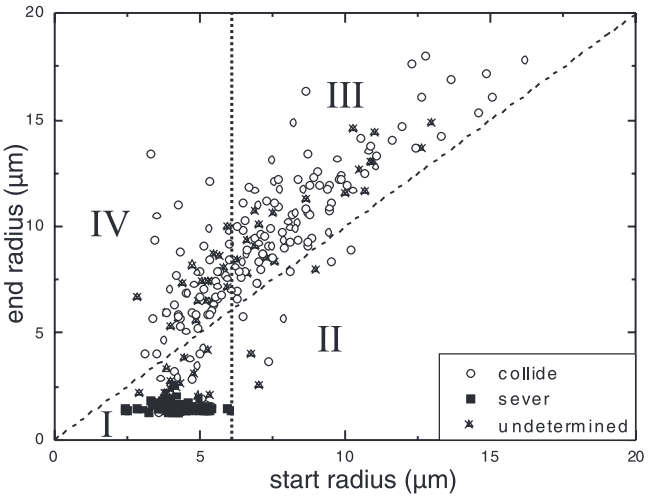

FIG. 6. Plot of bridge radius at the start of the track to the end of the track for tracks beginning before 1000 s. The dashed line represents $y = x$. The vertical dotted line indicates a critical radius, below which the Laplace pressure inside the bridge is positive, such that material is directed towards the wetting layers. Areas I-IV are discussed in the text. Over 300 datapoints are shown.

after the final image, we start a new track as this tube collides with the domain next to it (marked with a circle). We will discuss the coalescence of two domains in more detail later (see also Figure 8).

We summarize the behaviour of the circular bridging domains in the second stage of phase separation in Figure 6. Here, we consider tracks that last for at least 98 s, beginning between 280 s and 973 s. The tracks are categorised by the way in which we stop the track in the following manner: either the tube shrinks until the connection between the plates is severed, or the domains collide and a new track is begun. There is a third undefined category where domains diffuse out of the field of view, or small domains close to the minimum detection radius collide with another, making the distinction between severing and collision unclear. For completeness, we also show this category.

We plot the domain radius at the point the track is stopped against the radius at the start of the track. The dashed line represents the function $y = x$, i.e., there has been no change to the domain size. We observe that all domains, which shrink and snap (indicated by the filled squares in area I), have a starting radius significantly smaller than $d/2$, consistent with the Laplace pressure argument.[32,36] In fact, all domains for which the connection between the two plates becomes severed, have a starting radius $\lesssim 6\ \mu$m, indicated by the vertical dotted line. This is slightly smaller than $d/2$ and indicates that the longitudinal curvature of the tubes is strictly $1/(d/2 - d_w)$, where d_w is the wetting layer thickness.[33] Indeed, for $d = 18\ \mu$m and $d_w \sim 3\ \mu$m, we find that the critical radius is approximately $6\ \mu$m, in good agreement with the observations. Moreover, the plot also shows that if the starting radius is larger than this critical radius, the bridges almost always grow and hardly ever shrink: area II in the figure has only a handful of datapoints, in contrast with area III, and the change in their size is quite small. Furthermore, neighboring coalescence events will locally reduce the wetting layer thicknesses and thus modify the pinch-off criterion, which may explain why a few events end up in area II.

We observe that domains of any size may expand, i.e., even area IV contains data points. This may partially be due to problems in image analysis at early times, when domains are small and may coalesce, without an apparent change to its centre of mass. This means the track is not lost, and the domain may gain enough material to change the direction of flow between the wetting layers and the tube. Furthermore, the crossover from SDSD (stage 1) to the growth of individual domains by pressure gradients (stage 2) is not abrupt and takes some time. In Figure 1, we see in the xz images that structures may bridge the plates, appearing as identifiable domains in the xy images, before the curvature in the longitudinal xz direction is established. This process may sufficiently increase the radius of a small domain such that the ratio between longitudinal and transverse curvature is favourable by the time the system fully moves into the second stage of phase separation.

We can deduce additional information about the rate of domain growth from Figure 7, where we plot the number of domains and their area fraction as a function of time. We

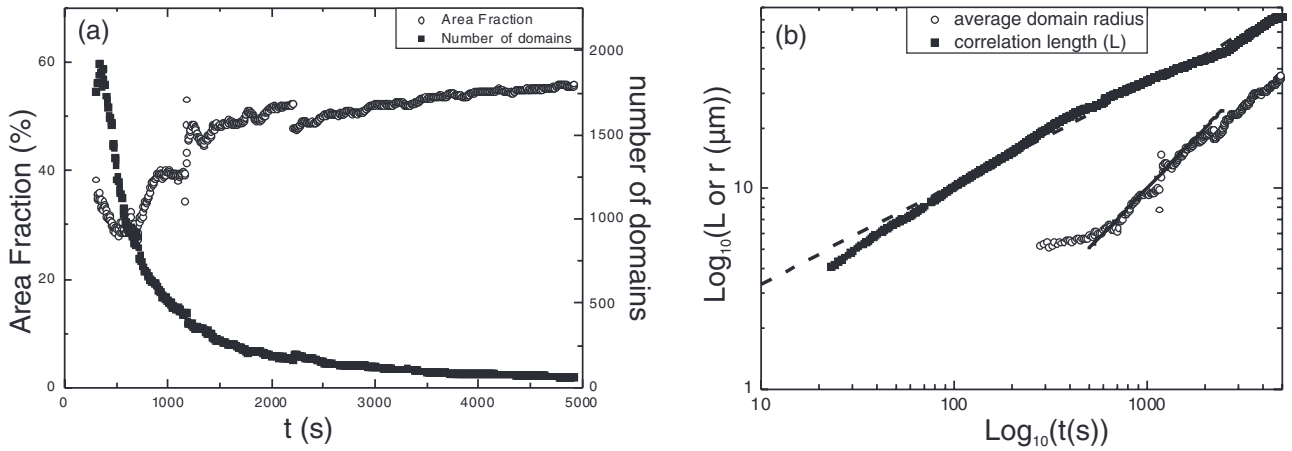

FIG. 7. (a) Analysis of coarsening domains in the confined xy plane—plot of area fraction and particle count with time. Note that the sudden jumps in the data happen when optimizing gain and offset settings on the CLSM. (b) Log-log plot of lengthscale vs. time for the correlation lengthscale and average domain radius in the system.

observe that the number of domains bridging the plates peaks at around 500 s, then decreases rapidly as the circular domains either collide, or shrink and disappear (Figure 7(a)). The rate of decay slows as domains become fewer in number and further apart. The area fraction of domains in the central *xy* plane is representative of the amount of material stored in the wetting layers—this value always remains less than the colloidal liquid-to-gas phase ratio of the system. We see that the value fluctuates until around 1000 s as smaller domains shrink and pump material into the wetting layers, while larger domains show the opposite behaviour. After this time, the area fraction of domains increases since remaining large domains draw material into the central plane to expand. This levels off after around 1500−2000 s as the wetting layer runs out of material.

The average radius $\langle r \rangle$ of the domains (Figures 4 and 7(b)) initially grows slowly as the curvature of the tubes bridging the plates is established. It then grows as $\langle r \rangle \sim t^1$ until around 2000 s, an exponent expected for such a hydrodynamic process.[23,36] As the domains collide and become interconnected rather than circular, the size is no longer represented by $\langle r \rangle$, but we continue to use $r = \sqrt{A/\pi}$ as an indication of the area change of individual domains. After 2000 s, we observe little expansion in individual domains (Figure 4) or increase in area fraction, however $\langle r \rangle$ still increases. This indicates that the system moves into the 3rd stage of phase separation, where coarsening is driven by the diffusion and coalescence of domains rather than the backflow of material from the wetting layers.

Even in the third stage, the diffusing domains may interact through the wetting layer. The Laplace pressure directs wetting phase material into the large domains; once the wetting layers begin to thin, adjacent domains will draw on the same material, pulling them together.[14,33] An additional attraction may be created by the capillary instability in a tube of non-wetting gas phase material in the area between wetting phase domains.[14] When the gap between domains is small, the domains deform and move to reduce the interfacial energy of this tube. When the domains coalesce, then this may leave a small droplet of the non-wetting phase inside the new larger domain. We show an example of such an event in Figure 8. A number of non-wetting phase droplets become trapped inside domains in the very late stages; these are relatively infrequent compared to the total number of coalescence events. In our system, we see very little deformation of domains prior to collision—domains become significantly more misshapen in the experiments of Tanaka.[14] This indicates that the attraction between domains in our system is of shorter range, which is directly related to the ultralow interfacial tension in our system. Furthermore, we speculate that the thermal capillary waves at the interfaces[50] may have an additional, reducing effect: the attraction is mediated by the curvature of the menisci in the *z*-direction, but in our case the menisci are constantly fluctuating. Although they form the expected semi-circular shape after time-averaging, it is clear from the snapshots in Figure 1 that the interfaces are rough on the micrometerscale, which is also the scale of the confinement and of the typical separation between bridges. This may lead to an entropic repulsion between two neighboring fluctuating interfaces, and will also locally and temporarily modify the pressure balance, which may well result in an additional reduction in attraction between neighboring bridges.

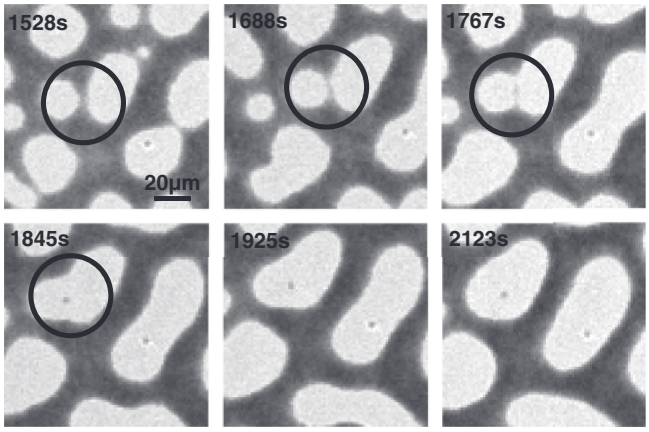

FIG. 8. Coalescence of two domains resulting in the formation of a droplet of the non-wetting phase.

In the third stage of coarsening, we expect domain growth to slow down.[33,34,36] We distinguish between the two lengthscales monitored in our system. The correlation length (L) is representative of the lengthscale of the gaps between domains[51] and the average domain radius is denoted by $\langle r \rangle$. We observe that $L \sim t^{1/2}$, surprisingly across all stages, and $\langle r \rangle \sim t^1$ in the second stage, slowing down as the system moves into the third. When backflow from the wetting layers stops driving domain growth, which would lead to a constant area fraction over time, we would expect the growth of these two lengthscales to be expressed by the same powerlaw. This disparity in addition to a small increase in the area fraction of domains at late times indicates that although coarsening is mainly driven by diffusion and coalescence, a small amount of backflow from the wetting layers remains present to the end of the experiment.

There is some discussion in the literature about the domain growth rate in the third stage of demixing, see, e.g., Ref. 14, 33, and 34. It is for example unclear if linear growth (t^1) crosses to diffusive growth ($t^{1/3}$) in the second and third stages, or grows logarithmically across both stages,[33] which is in contrast to our observed $L \sim t^{1/2}$ spanning more than two decades in time. We note that in Ref. 34, domain growth with thicker films does not slow down to a well-defined power law in the late stages, and wetting layer backflow continues to contribute to the coarsening. Observations may furthermore be hampered by a slow cross-over between regimes, as for example observed for bulk demixing.[40,52] Lastly, we note that differences in the interfacial properties of the systems studied may also lead to different strengths of interdroplet interactions, resulting in differing growth exponents. The observed $L \sim t^{1/2}$ growth is consistent with the droplet diffusion-coagulation mechanism in two dimensions based on Stokes flow,[53,54] although it would not be clear why such an exponent would be exhibited across all regimes. The appropriate growth laws for the spinodal decomposition of systems in thin film geometries has been explored in a large number of studies (for example, Refs. 55–58), however a consensus has not yet been reached, nor is it clear if a 2-dimensional

growth law would be applicable to our system and degree of confinement. We hope our data provide a stimulant for further simulation studies, which with the increase in computer power are probably best suited to address this issue.

IV. CONCLUSION

We have studied the demixing of a colloid-polymer system between two parallel plates, both of which are completely wet by the colloidal liquid phase. Our system exhibits 3 stages of phase separation: a 3-dimensional spinodal network, which coarsens into a system of 2-dimensional circular bridges between the two surfaces, and finally transforms into a partially interconnected network in two dimensions. During these stages, the system exhibits coarsening via SDSD, droplet growth/shrinkage driven by the Laplace pressure, and diffusion and coalescence. We have performed a detailed analysis of domain growth across the three regimes, including the tracking of individual domains bridging the plates, and obtained growth laws for each of the regimes. We find that the distinction between these regimes is not sharp, and our data suggest that more than one mechanism may take place simultaneously. Finally, we highlight two observations; first, our 3D real space images have enabled us to directly test the stability criterion for bridges spanning the two plates, and we find that bridges with a diameter smaller than the confinement length modified by the wetting layer thickness, may sever. Second, we observe that neighboring bridges only attract each other at small separations. We speculated that this may partially be attributed to a novel role of the thermal interface fluctuations, where the menisci in the system are more fuzzy and curvature-driven attractions are reduced, thus directly modifying the coarsening behaviour.

ACKNOWLEDGMENTS

We thank Thomas Skinner for his assistance in operating the IDL particle tracking program.

[1]E. Dickinson and P. Walstra, *Food Colloids and Polymers: Stability and Mechanical Properties* (Royal Society of Chemistry, Cambridge, 1993).
[2]R. A. L. Jones, L. J. Norton, E. J. Kramer, F. S. Bates, and P. Wiltzuis, Phys. Rev. Lett. **66**, 1326 (1991).
[3]G. Brown and A. Chakrabarti, Phys. Rev. A **46**, 4829 (1992).
[4]S. Puri and K. Binder, Phys. Rev. E **49**, 5359 (1994).
[5]K. Binder, Ann. Rev. Phys. Chem. **42**, 33 (1992).
[6]K. Binder, S. Puri, S. K. Das, and J. Horbach, J. Stat. Phys. **138**, 51 (2010).
[7]R. Evans, J. Phys.: Condens. Matter **2**, 8989 (1990).
[8]K. Binder, J. Horbach, R. L. C. Vink, and A. De Virgiliis, Soft Matter **4**, 1555 (2008).
[9]P. G. de Gennes, F. Brochard-Wyrat, and D. Quéré, *Capillarity and Wetting Phenomena: Drops, Bubbles, Pearls, Waves* (Springer, 2004).
[10]C. Gögelein, M. Brinkmann, M. Schröter, and S. Herminghaus, Langmuir **26**, 17184 (2010).
[11]M. Schmidt, A. Fortini, and M. Dijkstra, J. Phys.: Condens. Matter **15**, S3411 (2003).
[12]A. De Virgiliis, R. L. C. Vink, J. Horbach, and K. Binder, Europhys. Lett. **77**, 60002 (2007).
[13]G. Brown, A. Chakrabarti, and J. F. Marko, Phys. Rev. E **50**, 1674 (1994).
[14]H. Tanaka, Europhys. Lett. **24**, 665 (1993).
[15]E. D. Siggia, Phys. Rev. A **20**, 595 (1979).
[16]J. W. Cahn, J. Chem. Phys. **42**, 93 (1965).
[17]J. K. G. Dhont, J. Chem. Phys. **105**, 5112 (1996).
[18]D. G. A. L. Aarts, R. P. A Dullens, and H. N. W. Lekkerkerker, New. J. Phys. **7**, 40 (2005).
[19]J. W. Cahn and J. E. Hilliard, J. Chem. Phys. **28**, 258 (1958).
[20]I. Pagonabarraga, J.-C. Desplat, A. J. Wagner, and M. E. Cates, New. J. Phys. **3**, 9 (2001).
[21]G. Krausch, C.-A. Dai, E. J. Kramer, and F. S. Bates, Phys. Rev. Lett. **71**, 3669 (1993).
[22]S. Puri and K. Binder, Phys. Rev. A **46**, 4487 (1992).
[23]J. F. Marko, Phys. Rev. E **48**, 2861 (1993).
[24]M. Geoghegan, T. Nicolai, J. Penforld, and R. A. L. Jones, Macromolecules **30**, 4220 (1997).
[25]W. Straub, F. Bruder, R. Brenn, G. Krausch, H. Bielefeldt, A. Kirsch, O. Marti, J. L. Mlynek, and J. F. Marko, Europhys. Lett. **29**, 353 (1995).
[26]H. Tanaka and T. Araki, Europhys. Lett. **51**, 154 (2000).
[27]L.-T. Yan and X.-M. Xie, Macromolecules **39**, 2388 (2006).
[28]E. A. G. Jamie, R. P. A. Dullens, and D. G. A. L. Aarts, J. Phys. Chem. B **115**, 13168 (2011).
[29]G. Krausch, C.-A. Dai, E. J. Kramer, J. F. Marko, and F. S. Bates, Macromolecules **26**, 5566 (1993).
[30]M. Geoghegan, R. A. L. Jones, and A. S. Clough, J. Chem. Phys. **103**, 2719 (1995).
[31]H. Tanaka, J. Phys.: Condens. Matter **13**, 4637 (2001).
[32]J. Bodensohn and W. I. Goldberg, Phys. Rev. A **46**, 5084 (1992).
[33]H. Wang and R. J. Composto, J. Chem. Phys. **113**, 10386 (2000).
[34]M. J. A. Hore and M. Laradji, J. Chem. Phys. **132**, 024908 (2010).
[35]A. J. Bray, "Coarsening dynamics of nonequilibrium phase transitions," *Soft and Fragile Matter: Nonequilibrium Dynamics, Metastability and Flow* (SUSSP and Institute of Physics, 2000).
[36]H. Tanaka, Phys. Rev. Lett. **70**, 2770 (1993).
[37]S. Asakura and F. Oosawa, J. Polym. Sci. **33**, 158 (1958).
[38]A. Vrij, Pure Appl. Chem. **48**, 471 (1976).
[39]H. N. W. Lekkerkerker, W. C. K. Poon, P. N. Pusey, and A. Stroobants, Europhys. Lett. **20**, 559 (1992).
[40]E. A. G. Jamie, R. P. A. Dullens, and D. G. A. L. Aarts, J. Phys.: Condens. Matter **23**, 194115 (2011).
[41]E. A. G. Jamie, R. P. A. Dullens, and D. G. A. L. Aarts, J. Phys.: Condens. Matter **24**, 284120 (2012).
[42]E. Kumacheva, O. Kalinina, and L. Lilge, Adv. Mater. **11**, 231 (1999).
[43]G. H. Koenderink, D. G. A. L. Aarts, V. W. A. De Villeneuve, A. P. Philipse, R. Tuiner, and H. N. W. Lekkerkerker, Biomacromolecules **4**, 129 (2003).
[44]E. A. G. Jamie, G. J. Davies, M. D. Howe, R. P. A. Dullens, and D. G. A. L. Aarts, J. Phys.: Condens. Matter **20**, 494231 (2008).
[45]A. del Campo and C. Greiner, J. Micromech. Microeng. **17**, R81 (2007).
[46]Y. Xia, J. J. McClelland, R. Gupta, D. Qin, X.-M. Zhao, L. L. Sohn, R. J. Celotta, and G. M. Whitesides, Adv. Mater. **9**, 147 (1997).
[47]T. Hashimoto, T. Koga, H. Jinnai, and Y. Nishikawa, Nuovo Cimento **20**, 1947 (1998).
[48]J. C. Crocker and D. G. Greer, J. Colloid Interface Sci. **179**, 298 (1996).
[49]A. O. Parry, C. Ràscon, E. A. G. Jamie, and D. G. A. L. Aarts, Phys. Rev. Lett. **108**, 246101 (2012).
[50]D. G. A. L. Aarts, M. Schmidt, and H. N. W. Lekkerkerker, Science **304**, 807 (2004).
[51]J. H. J. Thijssen and P. S. Clegg, J. Phys.: Condens. Matter **22**, 455102 (2010).
[52]A. E. Bailey, W. C. K. Poon, R. J. Christainson, A. B. Scholfield, U. Gasser, V. Prasad, S. Manley, P. N. Segre, L. Cipelletti, W. V. Meyer, M. P. Doherty, S. Sankaran, A. L. Jankovsky, W. L. Shiley, J. P. Bowen, J. C. Eggers, C. Kurta, T. Lorik, Jr., P. N. Pusey, and D. A. Weitz, Phys. Rev. Lett. **99**, 205701 (2007).
[53]K. Binder and D. Stauffer, Phys. Rev. Lett. **33**, 1006 (1974).
[54]K. Binder, Phys. Rev. B **15**, 4425 (1977).
[55]M. S. Miguel, M. Grant, and J. D. Gunton, Phys. Rev. A **31**, 1001 (1985).
[56]H. Furukawa, Phys. Rev. A **31**, 1103 (1985).
[57]S. K. Das, S. Puri, J. Horbach, and K. Binder, Phys. Rev. E **72**, 061603 (2005).
[58]S. K. Das, S. Puri, J. Horbach, and K. Binder, Phys. Rev. E **73**, 031604 (2006).